PROPELLER DESIGN FOR PROPULSION AND REGENERATION

John Huisman, MARIN, The Netherlands
Jidde Looijenga, Rondal, The Netherlands
Mark Leslie-Miller, Dykstra Naval Architects, The Netherlands

SUMMARY

Regenerative sailing, also referred to as regeneration or hydro generation, is an efficient method of converting wind energy into electricity during sailing.

Two very different solutions on power regeneration were studied. Although each solution has its own field of application and associated cost and objective functions for optimization, this paper shows the applicability of the propeller optimization tool PropArt for different scenarios.

When the main propeller would be used for power regeneration, PropArt is able to optimize the propeller geometry for both propulsion and power regeneration mode. It appeared that, when operating in the third quadrant of propeller operation, the propeller geometry can be optimized for both propulsion and regeneration, without clear trade-off.

When a propeller is dedicated to regeneration only, all constraints concerning propulsion are not present. This allows smaller blade area and results in higher efficiency. The validation of the propeller design for the dedicated regeneration system with model tests showed a good match between computations and measurements, with a slightly better efficiency measured in the tests compared to computations.

The results and polynomials can be used for a better understanding of the potential output and the impact of regeneration of sailing yachts and ships.

1. INTRODUCTION

Regenerative sailing, also referred to as regeneration or hydro generation, is an efficient method of converting wind energy into electricity during sailing. There are several sailing yachts that use this technology to create electricity for hotel load or to charge batteries during sailing. Most of these yachts use the main propulsion propeller for this purpose. However, there is typically a significant penalty in drag and therefore ship speed. Regeneration efficiency plays a crucial role, since a loss of speed caused by the drag will reduce the electrical output.

In this paper, an overview is given of optimization computation software developed by MARIN, which is capable of optimizing propeller design with the additional objectives required for regeneration, complementary to other requirements and objectives of propeller design.

This paper includes two cases where this approach is applied: a propulsion thruster that can be turned 180 deg and function as a regeneration system for significant electrical output, and a dedicated regeneration system optimized for efficiency and a low drag when not in use.

The knowledge obtained by these cases and the optimized approach can potentially be used for more sailing yachts and ships and thereby result in more sustainable yachts which are less dependent on fossil fuel.

2. PROPELLER DESIGN

A propeller design is always a compromise and by using optimisation techniques, the best balance between the objectives can be demonstrated using Pareto front plots as shown later in Figure 5-1. All dots in the figure represent a particular propeller design. As the design process advances, better propellers are created. This is shown in the figure as going from the earlier designs in blue to the latest ones in red. The Pareto front is given by the propellers represented by the dark red dots.

Propeller computations were done with PROCAL, a boundary element method (BEM) which computes the inviscid flow around the propeller within the ship's wake field. Besides efficiency, the calculations give the pressure distribution and the extent including the dynamics of the sheet cavitation developing on the propeller blades. PROCAL has been developed by MARIN [2] within the Cooperative Research Ships (CRS) framework [3] and has been extensively validated. The input for PROCAL is an operational condition in terms of speed, thrust and rotation rate and the wakefield in which the propeller operates.

Within MARIN and the CRS, the multi-objective optimisation method PropArt has been developed for propeller design optimisation studies [4]. A parametric propeller geometry is coupled to an optimisation algorithm. PROCAL computations are performed for thousands of propeller geometries with varying radial distributions. After the PROCAL computations, often in multiple design conditions, the performance is evaluated in terms of cavitation behaviour, efficiency and strength requirements.

3. POWER REGENERATION

3.1 Definitions

The results in terms of propulsion are reported in terms of the well-known advance coefficient J, thrust coefficient K_T and torque coefficient K_Q. Propeller efficiency is defined as the ratio of the useful power and the required power. In propulsion the useful power is thrust times speed and the required power is the shaft power. For regeneration, however, the useful power is the shaft power, while the required power is the drag times speed.

For power regeneration, the results are typically presented as function of the hydrodynamic pitch angle β which is defined as

$$\beta = \arctan \frac{V}{0.7\pi n D} \tag{1}$$

with V the forward speed, n rotational speed and D the propeller diameter. The propeller thrust and torque, are made non-dimensional by the relative resultant velocity at 0.7R radius and defined as,

$$V_r = \sqrt{V^2 + (0.7\pi n D)^2} \tag{2}$$

The propeller thrust loading coefficient is defined as:

$$C_T = \frac{T}{(\frac{1}{2}\rho V_r^2)\frac{\pi}{4}D^2} \tag{3}$$

with T the thrust (or drag) of the propeller. The propeller torque loading coefficient is defined as:

$$C_Q = \frac{Q}{(\frac{1}{2}\rho V_r^2)\frac{\pi}{4}D^3} \tag{4}$$

With Q the torque of the propeller. Then, the regeneration efficiency can be written as:

$$\eta_{regen} = \frac{P}{VT} = \frac{C_Q}{C_T}\frac{2}{0.7\tan(\beta)} \tag{5}$$

with $P = 2\pi n Q$ the power of the propeller. Finally, the power coefficient is defined as

$$C_P = \frac{P}{P_{flow}} = \frac{2C_Q\left(1+\frac{1}{(\tan\beta)^2}\right)}{0.7\tan\beta} \tag{6}$$

With flow power $P_{flow} = \frac{1}{2}\rho V^3 \frac{\pi}{4} D^2$. The flow power is the potential energy in the flow that streams through the propeller disk.

3.2 Tuning with model scale data

A feasibility study was performed whether the computational tool PROCAL, as used for propeller design, is also suited to compute the performance in terms of thrust and power in the envisioned range of operation of the propellers during regeneration. This study showed that PROCAL was suited with sufficient accuracy.

Tuning was done based on the measurements within the recent Wageningen F-series Joint Industry Project (JIP). This data is still confidential within the JIP, and cannot be shown in this paper yet.

3.3 Propeller quadrants

The left of

Figure **3-1** visualizes the propeller operation as function of the angle of attack. This is divided in four quadrants. While being the easiest to generate power in the first quadrant Q1, the third quadrant Q3 would provide significantly higher efficiency. In the first quadrant the propeller operates with the leading edge first, while in the third quadrant the trailing edge becomes the leading edge. In the third quadrant the camber of the blade profiles is aligned with the flow direction. This is more efficient compared to the first quadrant in which the camber is in the wrong direction. The propeller is then operating in its so-called third quadrant with - from the propellers point of view - a negative rate of revolutions and negative ship speed. Operating in the third quadrant means that the trailing and leading edge switch, meaning that the leading and trailing edge should be designed as combined leading and trailing edge.

The right of

Figure **3-1** compares the regeneration performance in the first and third quadrant in terms of C_P and η_{regen} as computed on the rear propeller of project Zero [1]. As shown, both efficiency and power coefficient are better when operating in Q3.

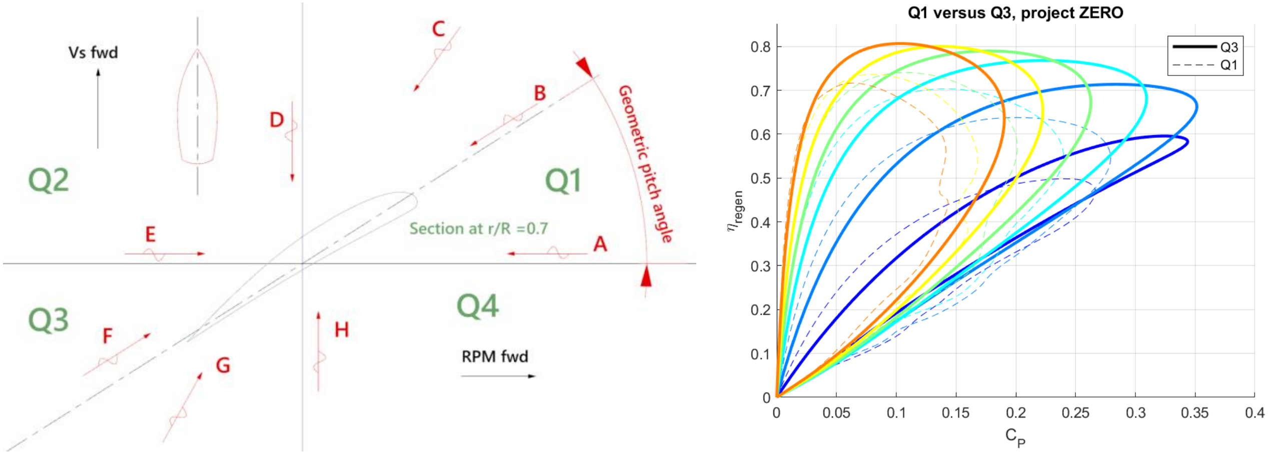

Figure 3-1: *Left: Quadrants and working points of a propeller. A: Bollard pull condition, no speed. - normal propulsion between A and B. B: Zero thrust condition. C: Hydro generation in first quadrant. D: No RPM, fwd speed, propeller in drag mode. - between D and E the angles of attack are too large to be useful. E: Bollard pull in reverse condition, no speed - reverse propulsion between E and F. F: Zero thrust condition G: Hydrogeneration in third quadrant. (assuming boat speed aft or 180° rotation of pod). H: Reverse speed, 0 rpm, prop in drag mode. - between H and A the angles of attack are too large to be useful. Right: Comparison of regeneration in the first and third quadrant*

4. COMBINED PROPELLER DESIGN FOR PROPULSION AND REGENERATION

The first case study is to design an optimized all-round propeller, suited for power regeneration and propulsion, for sailing yacht Project Zero. The sailing yacht is being equipped by two pushing thrusters with controllable pitch propellers without ducts, a smaller one before the keel primarily optimised for regeneration, and a larger unit after the keel, primarily optimised for propulsion. Power will be generated while the azimuth thruster is turned around, to efficiently operate in the third quadrant.

On behalf of Foundation Zero, Dykstra Naval Architects commissioned MARIN to study the two thrusters for the sailing yacht Zero. Project Zero is focused on the development of a sail yacht that is entirely independent on the

use of fossil fuels in its operation. The yacht is powered solely by renewable energy, harvesting heat and electricity from the sun and collecting the energy that is generated by sailing via the propulsors.
The objective for MARIN was to determine the performance of both thrusters while generating power under sail, and the performance during propulsion. Two main questions were addressed:
1. Is it feasible to harvest 250 kW power at 16 kn ship speed?
2. How to design a Controllable Pitch Propeller (CPP) propeller for both propulsion and regeneration?

Operational scenarios were provided by Dykstra. The ship is powered by sails and propellers which can be used in different combinations:
1. Maximum regeneration with both props at 16 kn ship speed with an expected total power generation of 250 kW.
2. Intermediate speed motoring for short stretches, delivered by one or two propeller; to be investigated what combination is best. Ship speed of 12 kn, at an approximate power of 380 kW.
3. Regeneration mode with both props active at 14 kn ship speed with expected total power generation of 125 kW.
4. Light regeneration by the front propeller only and the aft propeller probably feathered. The ship speed is 10 kn and the regenerated power is 20 kW. At ship speeds over 10 kn, the aft propeller would probably be used for regeneration as well.
5. Free sailing with both propellers feathered at a ship speed of 8 kn.
6. Motorsailing on the aft propeller, front propeller either feathered or lightly driven to reduce drag. The ship speed is 10 kn and the total propulsion power is 50 kW.
7. Economic motoring for maximum range (no wind) on the aft propeller, with the front propeller either feathered or lightly driven to reduce drag. Ship speed is 8 kn, at an approximate power of 100 kW.
8. Maximum power on both propellers in bollard pull condition in order to sail away from a lee-shore.

4.1 Initial investigations

Propeller manufacturer Hundested provided preliminary designs of both propellers and thrusters. The first objective was to assess the performance of both Hundested thrusters and propellers in both propulsion and regeneration mode according to the operational scenarios as provided by Dykstra.

Since the propellers are CPP, one of the tasks is to find the optimum rotation rate and optimum pitch for each condition. To do so, a polynomial description of propeller performance is required. Therefore, CFD computations were performed using RANS-BEM to obtain the wake fields of the ship and thrusters both in regeneration and propulsion. For propulsion, the wake field was determined with feathered front propeller. Hull efficiency was studied. The suction in propulsion and stagnation in regeneration of the propeller should affect the resistance of the ship as little as possible, while the inflow velocity should be as high as possible for power regeneration and as low as possible for propulsion.

Further, CFD computations were performed using RANS-BEM on both thrusters to determine the open water characteristics, both in propulsion and regeneration mode. Based on this data, polynomials as function of propeller pitch and advance coefficient for both propulsion and regeneration mode were determined for both thrusters. Using the polynomials design points were determined in terms of propeller pitch and propeller rotational speed for both propulsion and regeneration.

Dykstra integrated the polynomials in their performance prediction programs to study the optimum combination of pitch and rotation rate in each voyage simulation.

Using computational tools MARIN analysed the performance of the propeller designs in terms of powering, regeneration and cavitation behaviour. It appeared that both in propulsion and regeneration the designs features quite some cavitation and the strut of the unit would show flow separation. Therefore it was decided to optimize both the propellers and the struts of the thrusters.

4.2 Propeller design optimization

The propeller designs were optimized using PropArt [4], using the CMO-PSO algorithm by Zhang et al. [5]. The goals were twofold: the first is the minimization of the required power in propulsion, and the second is the maximalization of the harvested power in regeneration. A fixed ship speed, propeller rotation rate and thrust was selected for both conditions. Constraints were added to the optimization problem, for strength, flow separation, cavitation margins and extent, under water radiated noise and pressure excitation on the ship hull.

The geometry of the propellers was fully parametrised in both the radial and chordwise geometry distributions using Bezier curves, as shown in Figure 4-1 to Figure 4-3. The distributions for rake and maximum thickness follow a similar recipe. The control points of the Bezier curves serve as the optimisation variables. Quite some variations are possible. The task of the optimiser is to find the most optimal distributions. The diameter of the propellers was not varied in this study.

Especially for the blade profiles (chordwise camber and thickness distributions) the parametrisation was adapted with the purpose of regeneration in mind. The trailing edge (normally just finite thickness) is now regarded as leading edge for regeneration. The basis profile is symmetric in terms of thickness and camber. The optimiser will select the direction to tune, either favourable for regeneration or propulsion, or both simultaneously.

In total the parametrisation consist of 58 design variables, which makes this a very extensive optimisation problem. The blade profiles are defined at the root and a mid-radii (also a design variable) and the tip, in between which the profiles are interpolated.

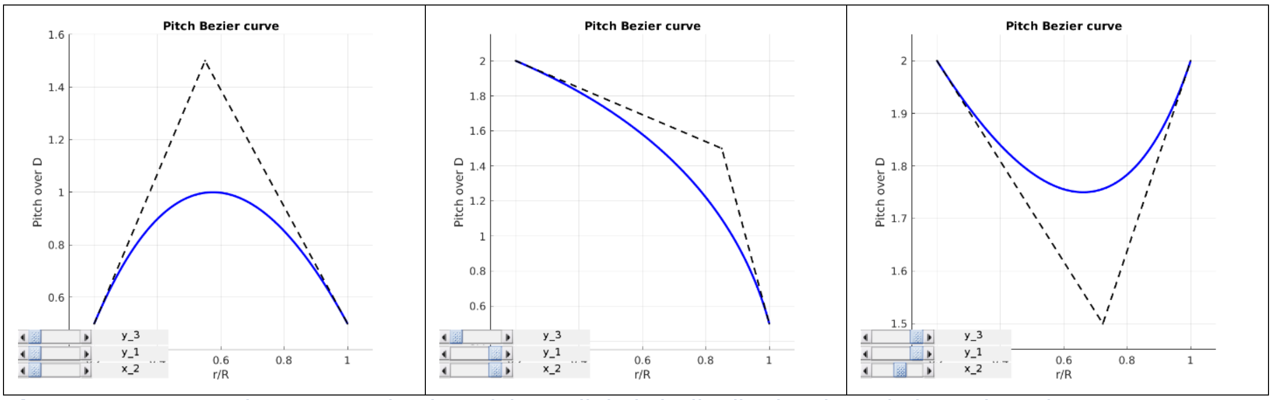

Figure 4-1: *Bezier parametrisation of the radial pitch distribution (3 variations shown).*

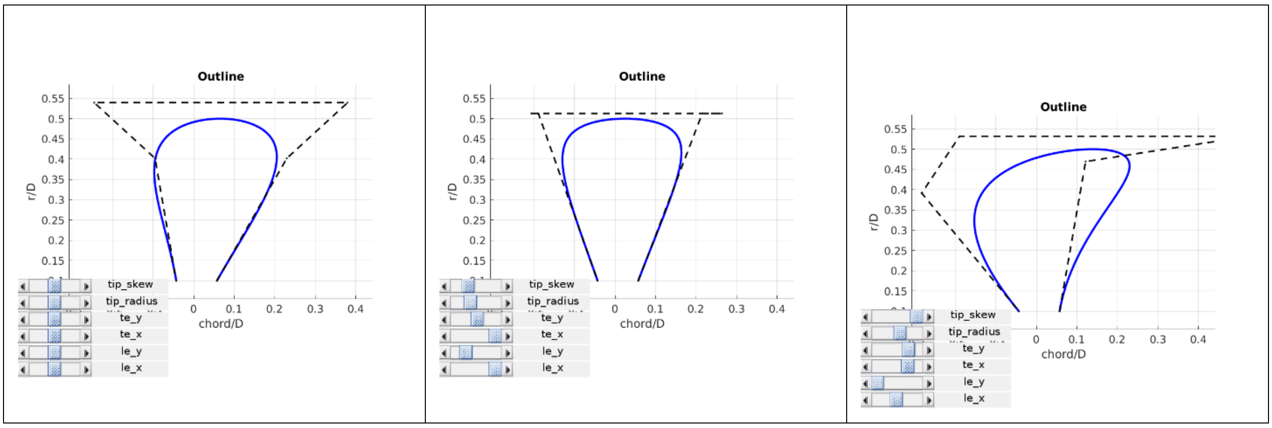

Figure 4-2: *Bezier parametrisation of the radial outline (skew and chord) distribution (3 variations shown).*

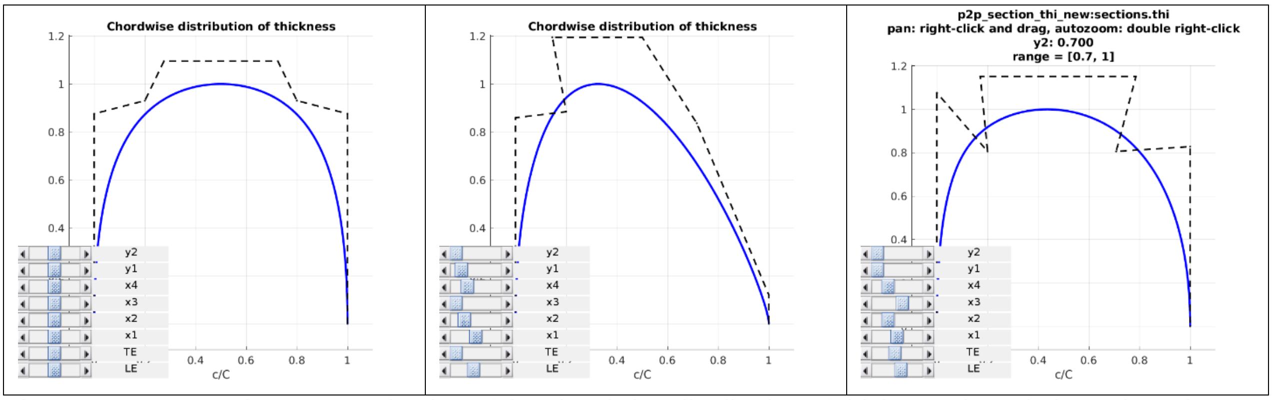

Figure 4-3: *Bezier parametrisation of the chordwise distribution of thickness (3 variations shown).*

While designing both edges hydrodynamically, a point of attention is propeller singing. A normal propeller features an anti-singing edge at the trailing edge. In view of the usage of the trailing edge in regeneration it is not advised to apply an anti-singing edge, although this increases the risk on propeller singing in propulsion. Propeller singing in regeneration remains a risk.

In total 6 PROCAL computations are done for each individual: 3 in generation mode and 3 in propulsion mode. One computation to set the pitch, one in an overloaded situation, and one to analyse flow separation which is done using a steady (averaged) computation.

The optimization was approached using several iterations, to optimise the propulsion efficiency, regeneration efficiency and cavitation performance. Based on the results, the optimisation objectives are evaluated. Each optimization run gives Pareto Fronts. It appeared that optimizing for regeneration performance was also beneficial for propulsion performance. No clear trade-off was found. In MARIN's opinion the currently optimised propellers feature a good balance between efficiency and cavitation nuisance in view of the yacht type of application which comes with high comfort standards.

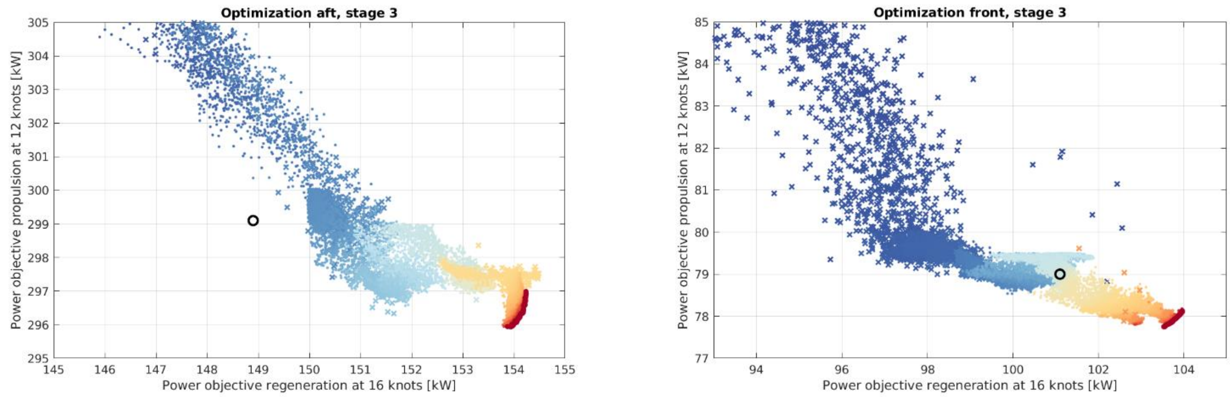

Figure 4-4: *Optimization results, converging from blue to red. The black circle is the reference design.*

4.3 Strut optimization

The design of the thruster strut and housing was optimized for minimum drag around the required structure and mechanics. In this design, - as for the propellers - a deliberate choice was made to optimize the front thruster for generation and the aft one for propulsion. For the second analysis round, the shape of the legs was adjusted to reduce separation and improve the flow into the propeller disk. This could be combined with a reduction in drag in feathered (free sailing) mode.

FWD THRUSTER

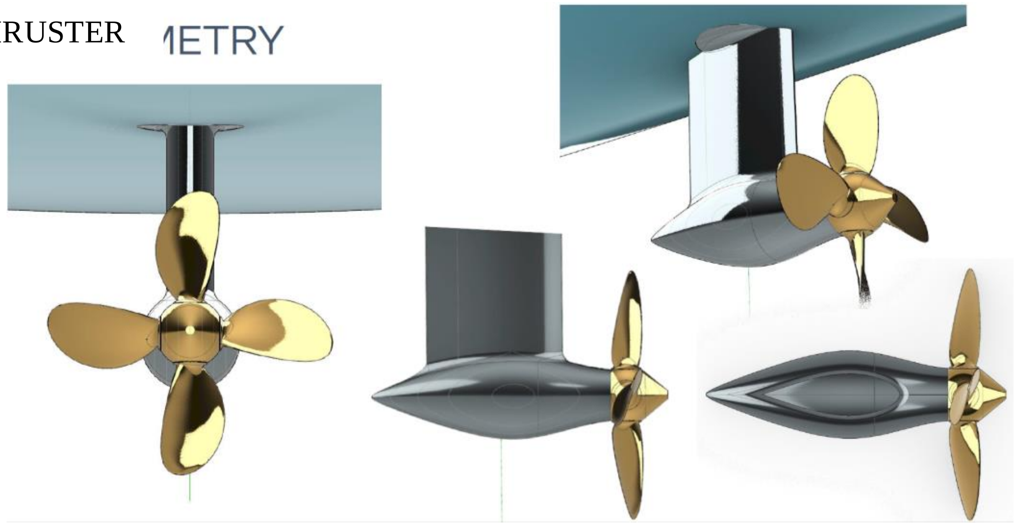

Figure 4-5: Front thruster overview

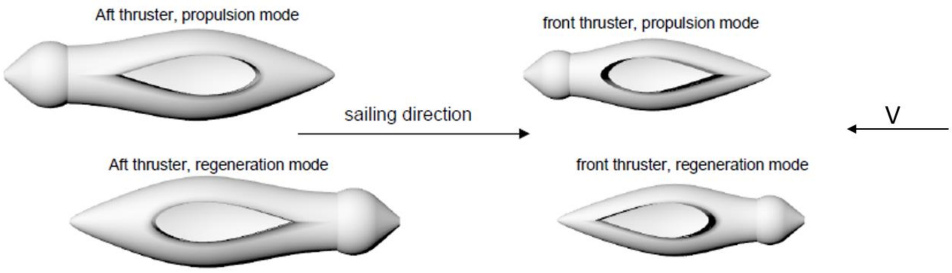

Figure 4-6: Modes of operation for front and aft thruster

4.4 Final assessment

Propeller manufacturer Hundested checked the optimized propeller designs for practical issues. The final propellers are largely based on the proposal for optimized propellers as given by MARIN, with small modifications in rake and skew to fit the hub. The RANS computations on the hull and in open water were done again, the hull interaction was studied and new polynomials were generated. A visualization of the polynomials is provided in Figure 4-7. The regeneration efficiency includes the drag of the thruster.

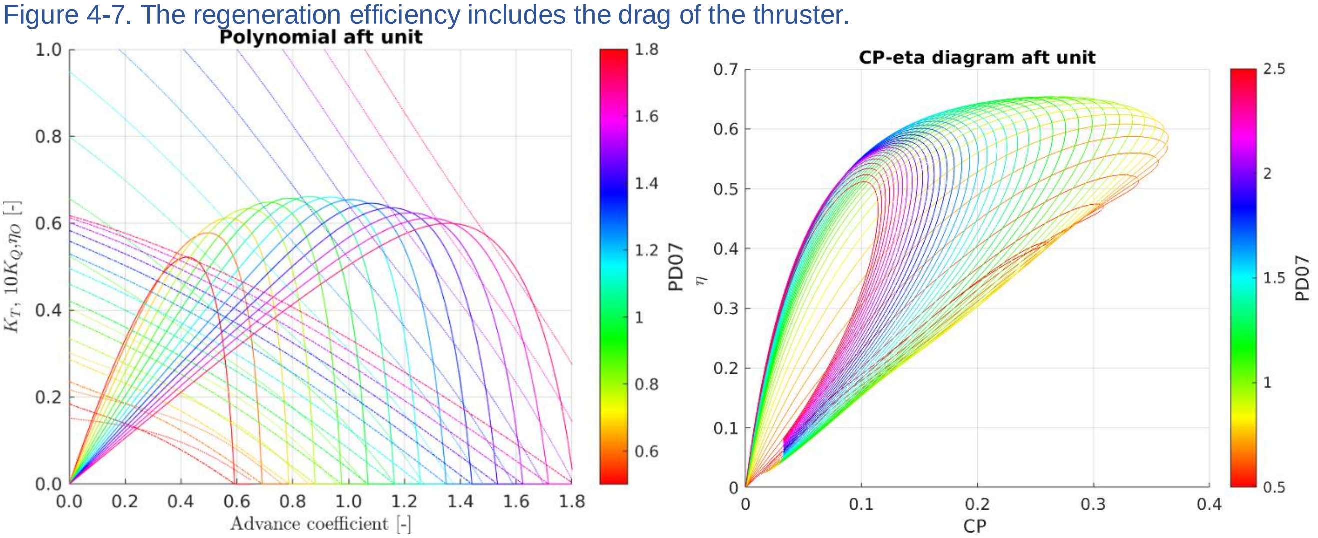

Figure 4-7: *Polynomials of performance in propulsion (left) and regeneration (right)*

A comparison of the cavitation behaviour for the aft propeller is provided in the sketches in Figure 4-8. The original propeller (v1) featured quite some sheet cavitation in propulsion at 12 kn (12kn_ff), while also quite some sheet cavitation was present in regeneration at 16 kn (16kn_250). The optimized propeller design (v2) has clearly reduced extent of sheet cavitation in both conditions. The reduced extent of cavitation also reduces the pressure excitation on the hull, thereby reducing the risk on noise and vibrations.

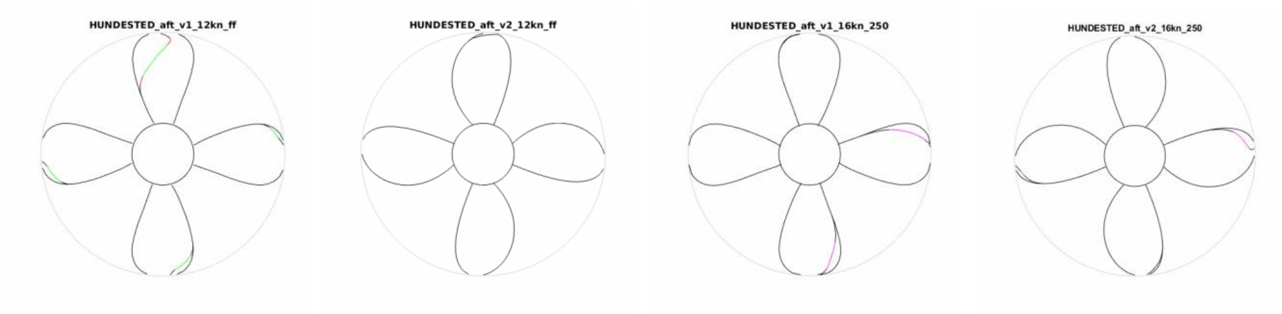

Figure 4-8: *Comparison of cavitation performance for the initial designs and optimized designs.*

The new propellers can operate at higher efficiency and higher CP, such that they can harvest more energy. A comparison is provided in Figure 4-9, for both the aft and front thruster. The propeller efficiency ETAp is provided as well as the unit efficiency ETAu, which includes the drag of the thruster.

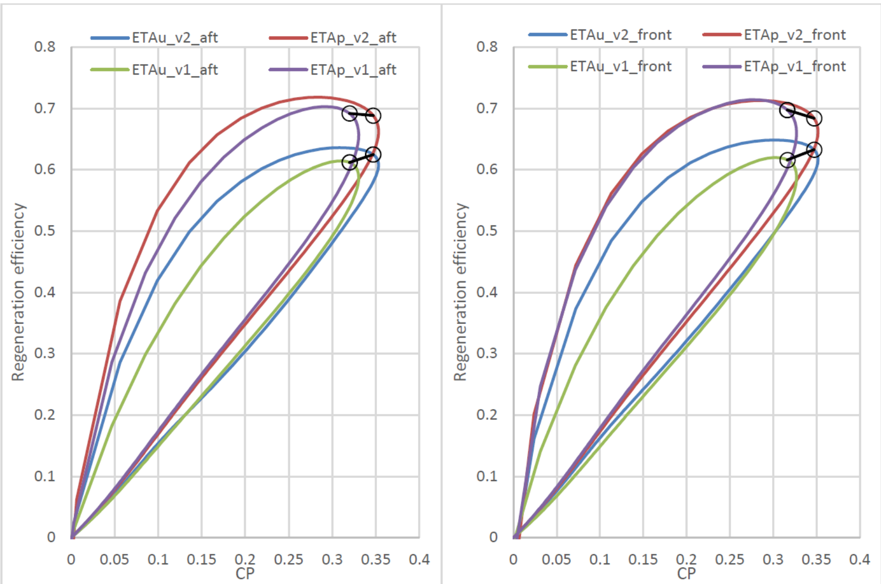

Figure 4-9: *Comparison of initial (v1) and optimized (v2) geometries for Project Zero*

However, the total regeneration efficiency was improved less than expected due to a less favourable interaction of flow from the front propeller with the aft propeller. Less flow separation was present, which gave a more stable jet from the front propeller such that the aft propeller encountered lower flow velocities and could therefore harvest less energy. Due to the change in operational conditions, the cavitation behaviour was also different than expected. Nonetheless, due to the robust design, the propellers were able to cope with this.

Although the aft propeller could harvest less, the hull resistance improved considerably. Finally, the regeneration efficiency at 16 kn was still improved such that the total resistance reduced with 5% compared to the first geometry variant when generating 250 kW of power. Finally, also during propulsion, up to 10% reduction in required power was predicted for propulsion, depending on the operational mode.

The results of this project are also very valuable for other parties that consider power regeneration for sailing yachts. The polynomials enable exploration of the possibilities of power regeneration and the corresponding drag, optimum diameter and rotation rates. The polynomials are available in report 32992-2-POW from MARIN, which is available on the website of Foundation[0] [1].

5. PROPELLER DESIGN FOR DEDICATED REGENERATION

The second case study is a dedicated propeller design for power regeneration. Rondal, part of the Royal Huisman Group, is a supplier of sailing systems for large sailing yachts. Since regeneration is a unique feature for sailing yachts, Rondal has decided to develop a dedicated regeneration system which does not have any propulsion requirements. The purpose of this regeneration system is to supply energy for the hotel load and energy during sailing, reducing the reliability on stored (fossil) energy during sailing under sail. Compared to the combined propulsion and regeneration system of the first case, this system is smaller and can be applied on yachts with conventional propulsion systems.

The dedicated regeneration system has an e-motor that is integrated in a pod, a gearbox and a fixed pitch propeller. There are no demands for propulsion or bollard pull. Experience from existing combined propulsion and regeneration systems shows that in general the willingness to use regeneration decreases when it influences the sailing speed too much. Therefore, the focus for this case was to optimize for efficiency rather than a large output. The output objective was about 15 kW at a ship speed of 15 kn.

5.1 Design points

The propeller diameter, propeller pitch and gear ratio were varied and the results were considered in terms of efficiency, power regeneration, torque and rotation rate. Mechanical or electrical efficiencies were not taken into account in this study. The power that is presented is merely the hydrodynamic power from the propeller. Four design points were selected, and their corresponding goals were defined:

1. 16 kn at maximum torque and maximum rpm: pitch basis; cavitation to be balanced.
2. 16 kn freewheeling: cavitation to be balanced.
3. 15 kn at maximum torque: power and efficiency to be maximised; cavitation to be balanced.
4. 12 kn at maximum torque: power and efficiency to be maximised; cavitation to be balanced.

A ship speed of 16 kn would be the maximum speed of operation. In the absence of a constant power region in the engine diagram due to the gear box rotation rate constraint, the full power of 17 kW can only be harvested at 16 kn. This is a severe limitation of the potential of the electromotor. This stresses the importance of a careful selection of the electric motor and corresponding gear box.

5.2 Computations and optimization

Propeller design tool PropArt was used. Using multiple optimisation runs, the optimum diameter and pitch were established. Also the chord, skew, rake, pitch, thickness and camber distributions were optimised for the best performance. Industry-standard blade profiles were applied for high efficiency performance. Figure 5-1 presents a summary of the optimisation results.

Propeller design optimisation is typically approached in different runs, in which iteratively the design space, objectives and constraints are modified until the optimisation results are satisfactory. The results of some optimisations runs are omitted which were merely checks or intermediate results.

A propeller with three and four blades was investigated. In this case, the performance difference was found to be negligible and it was decided to continue with a three-bladed propeller. A two-bladed propeller was not studied.

It appeared that cavitation limits clearly influence the design, not only in the required blade area ratio, but also in the thickness of the blade sections. Pressure side cavitation is critical in freewheeling situation, while suction side cavitation becomes present at 12 kn when regenerating at maximum torque.

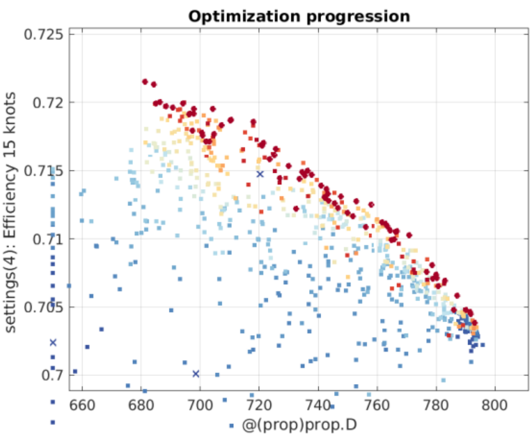

Run7: Efficiency at 15 kn versus propeller diameter

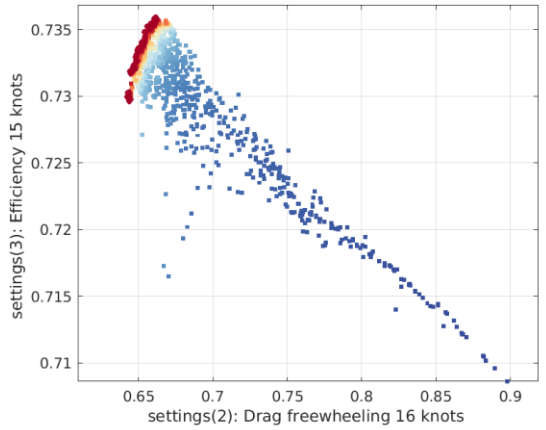

Run9: Trade-off between unit efficiency and drag free wheeling

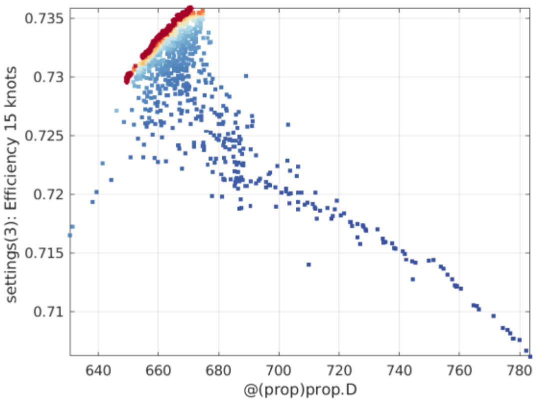

Run9: Trade off between diameter and unit efficiency in later stage of optimisation

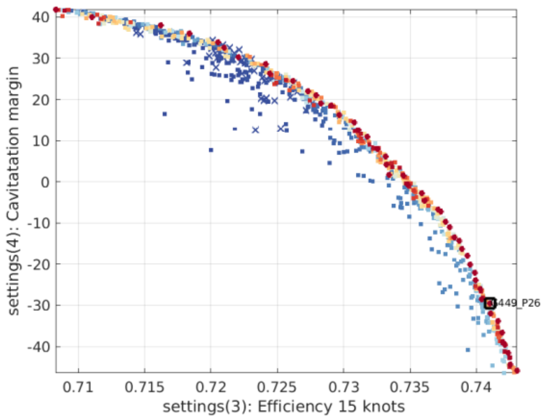

Run14: Restart upon the results of run 9 with slightly modified cavitation constraints and updated design input

Figure 5-1: *Summary of optimisation results.*

During the later optimisation runs the focus was to minimise the drag freewheeling and to optimise the efficiency at 15 kn. The efficiency at 12 kn is a result, rather than an objective. At 12 kn there would be a clear optimum efficiency region of operation, which would then not be at the maximum torque, but at lower torque. This can be understood when checking the propeller curves and engine diagram in Figure 5-6.

As shown in Figure 5-1, the optimisation results show a clear optimum for the diameter at 0.67 m. Hence, the final optimisation run was performed while fixing this diameter, optimising for the efficiency at 15 kn and the cavitation margin at 13 kn. This suction-side cavitation margin dominates the set of constraints, together with the pressure-side cavitation margin at 16 kn freewheeling. As good practise, the pressure-side margin was chosen to be about zero, to just avoid pressure side cavitation. This was implemented as constraint, while the suction side margin was used as objective.

Finally, individual 449_26 was selected from run 14 for further checks. The computed pressure distributions and cavitation extent is visualised in Figure 5-2. At 13 kn maximum torque a narrow band of cavitation was computed which is considered as a good balance between efficiency and amount of cavitation. The results are presented using the normalised pressure coefficient CPN and cavitation inception number σ_N, which are defined as:

$$\mathrm{CPN} = \frac{p-(p_a+\rho g h_s)}{\frac{1}{2}\rho n^2 D^2} \quad \text{and} \quad \sigma_N = -\frac{p_v-(p_a+\rho g h_s)}{\frac{1}{2}\rho n^2 D^2} \tag{7}$$

with p pressure, p_a the atmospheric pressure, $\rho g h_s$ the hydrostatic pressure at the shaft depth, p_v the vapour pressure, ρ water density, n rotational speed and D the propeller diameter. Using this definition, CPN can directly be compared with the cavitation number σ_N in the calculations. If -CPN equals or exceeds σ_N (p equals or exceeds p_v), then inception of cavitation occurs and the cavitation extent is computed.

As shown in Figure 5-2 the blade is very narrow with near constant chord length over the span of the blade. The thickness, however, decreases gradually towards the tip.

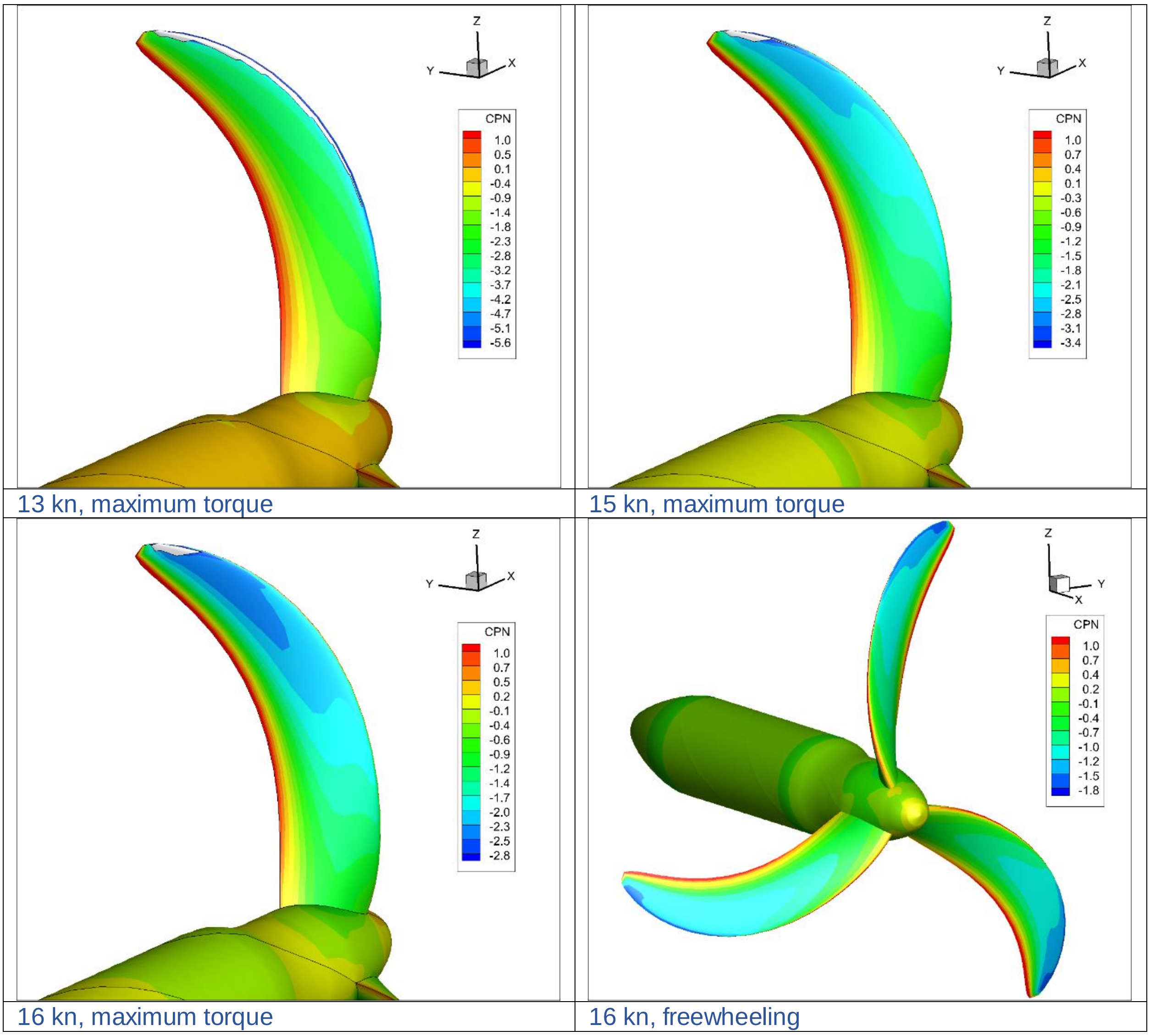

Figure 5-2: *Computed pressure distributions (contour) and cavitation extent (white shade).*

5.3 Model tests

The blade outline and chord length are outside the normal range of propellers. Therefore, to validate the computational results, model tests were done. It was chosen to perform tests with the standard open water setup, instead of having the complete unit of the pod. The linear scale ratio of the propeller was established at λ = 2. As such, the shaft of the measurement pod reproduces the diameter of the pod very well. The stream piece, hub and cap were reproduced to represent the real geometry on the pod.

Propeller individual 14_449_26 from the optimisation results was manufactured in bronze. Figure 5-3 shows two photographs of the propeller, propeller cap and the stream piece.

For each test run, both the towing speed of the carriage Va and the rotation rate of the shaft n are varying simultaneously and linearly (increasing or decreasing to a maximum or a minimum value) in a trapezoidal form as sketched in Figure 5-4, including starting, transition and stopping. As such the performance is determined quasi steady [6].

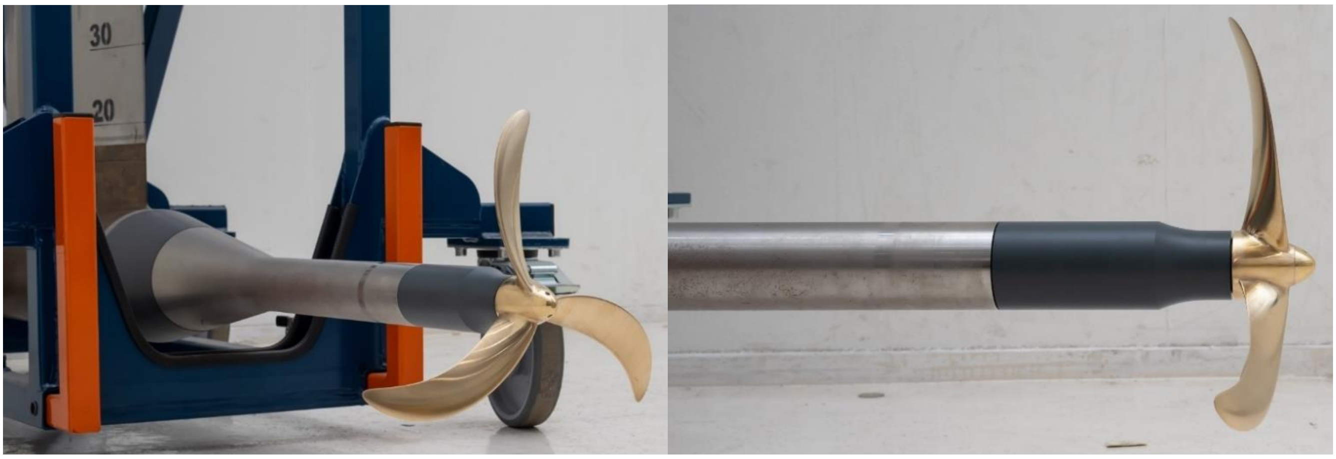

Figure 5-3: *Photographs of the manufactured propeller, including cap and stream piece.*

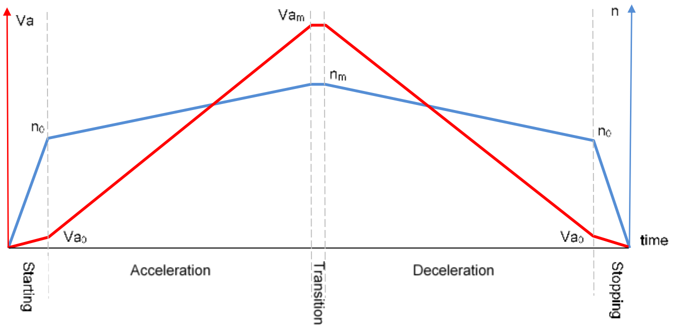

Figure 5-4: *Trapezoidal variation of advance speed Va and rotation rate n (example only).*

Three constant ship speeds were considered (Va0 = Vam), with varying rotation rate. Figure 5-5 shows the performance as function of β. The β in which power generation is most efficient is between -160 and -155 deg. Smaller than -160 deg the rotation rate is higher than optimal and friction becomes dominant. Larger than -155 deg, the rotation rate becomes lower than optimal, and the flow starts to separate from the blade, causing a reduction in efficiency. Flow separation is sensitive to Reynolds number, which is why there still is quite some difference between the tests. As shown, the lowest speed that was model tested, 3.63 m/s, has significant lower efficiency compared to the higher speeds. The 5.45 m/s and 7.00 m/s are close together in the relevant area in which the flow is properly attached to the propeller blade. This is the top part of the curve, starting from 0,0 towards maximum CP. This gives confidence that the results from 7.00 m/s do not suffer from significant scale effects anymore in the intended operational range. The results of 7.00 m/s are as such suitable to be used for full scale predictions. Only for smaller propeller diameters, at lower rotation rates and ship speeds (ship speed lower than 10 kn), scale effects become important.

The results of the model tests can be used to predict the hydrogenated power at a certain ship speed and propeller rotation rate, the corresponding drag and the drag during freewheeling when no power is generated.

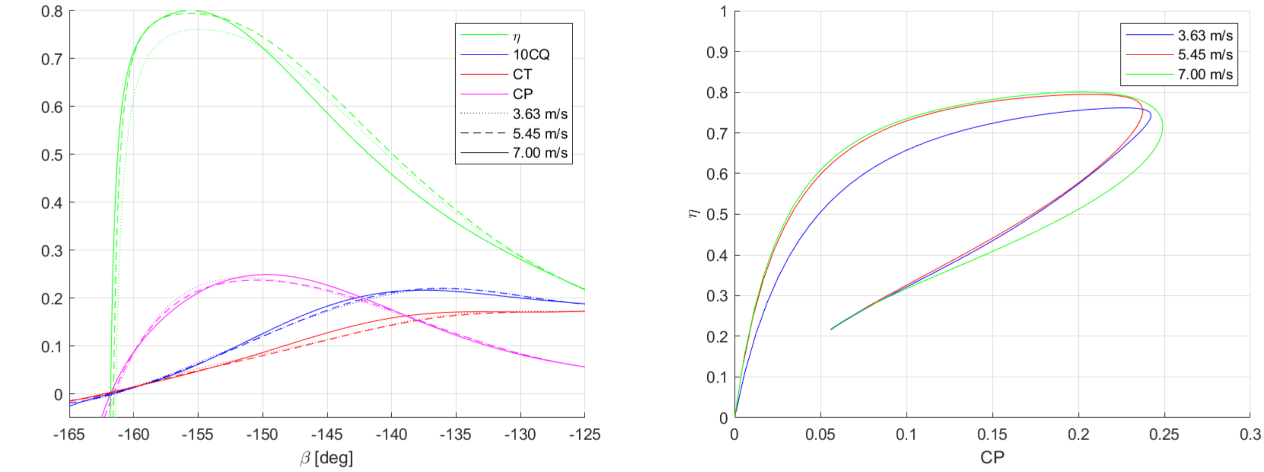

Figure 5-5: *Speed dependency on propeller efficiency η and power regeneration CP at model scale 2.*

5.4 Evaluation and comparison

In comparison to the computed performance, the measured performance is evaluated. The same correction for the resistance of the pod was applied as used in the computational phase. As such, the propeller efficiency is correctly compared. As shown in Figure 5-6 there is an excellent match concerning the dependency between rotation rate and ship speed. The pitch of the propeller matches the design point. The measurements show higher efficiency, up to 0.753. At 15 kn, the propeller operates at nearly optimum efficiency. A shaft power of 15.73 kW is generated at 15 kn ship speed at an efficiency of 0.750 and a rotation rate of 715 rpm. At 16 kn, both maximum torque, maximum power and maximum rpm are achieved.

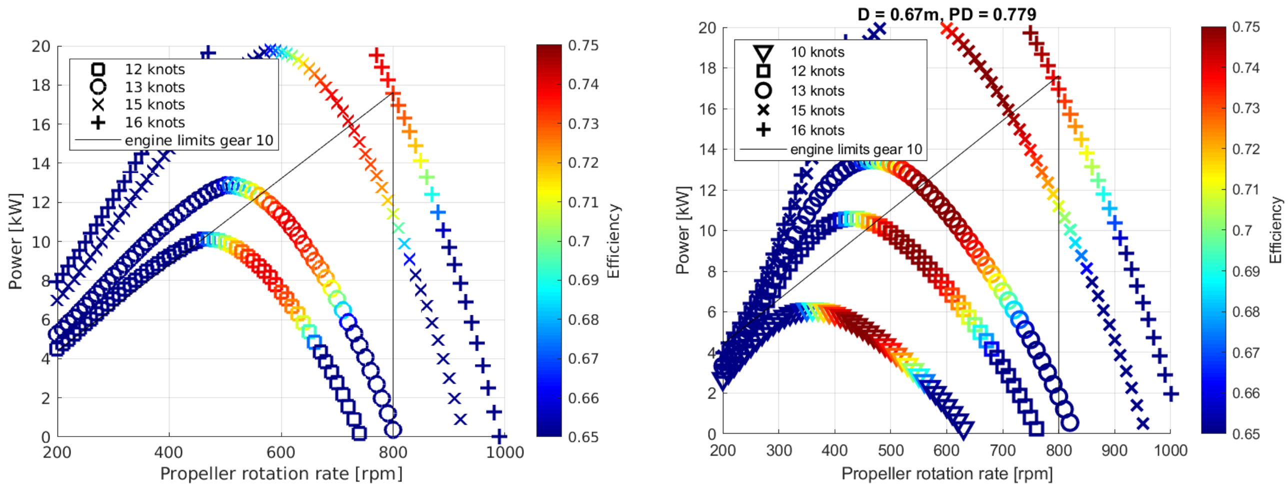

Figure 5-6: *Propeller curves and engine limits, computation (left) and measurement (right). Unit efficiency.*

Finally, Figure 5-7 shows the power versus drag curves at four ship speeds. The freewheeling drag, when no power is generated, is slightly over predicted by the computations. The measurements indicate that at 16 kn a drag of about 550 N should be accounted for. At a ship speed of 12 kn the drag during freewheeling is 300 N, including the estimated drag of the thruster unit, at a rotation rate of 763 rpm.

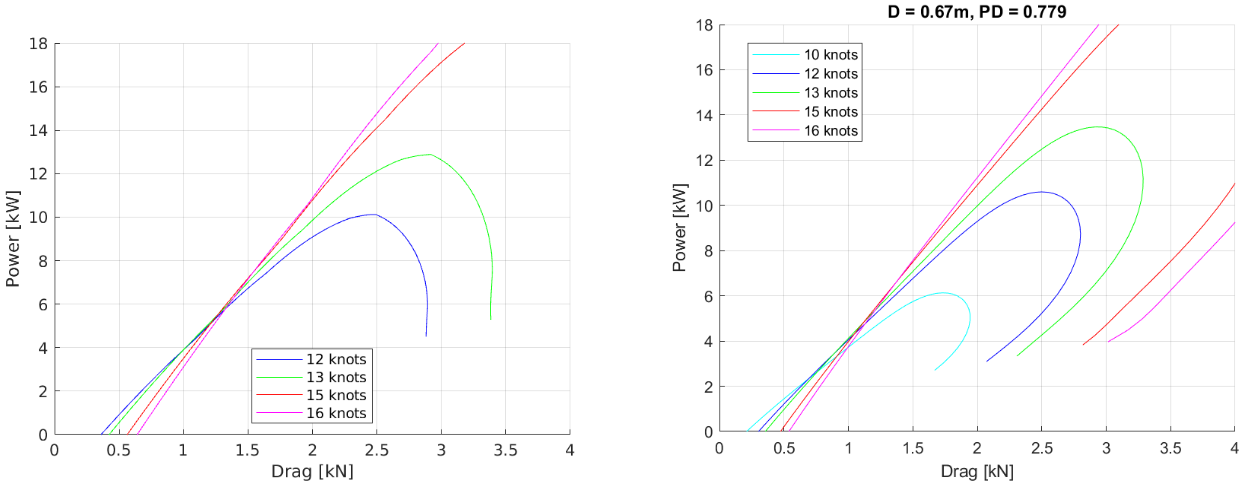

Figure 5-7: *Propeller power versus total drag, computation (left) and measurements (right)*

5.5 Second study

In addition to the development of the propeller with an output of 17 kW at 16 kn, a second propeller was developed by MARIN for a smaller pod, intended for yachts smaller than 45 m, with a lower hotel load requirement and lower top speed. The design objectives for this study were established as:

- Reduce drag in freewheeling at 10 kn
- Optimize power output in the range of 9 to 12 kn ship speed
- Achieve at least 8 kW at 11 kn ship speed.

Several propeller diameters were computed to optimize drag reduction. It appeared that a smaller diameter propeller would need a smaller pitch to achieve the required output, leading to a higher drag and lower efficiency. Therefore the same propeller diameter of 670 mm was chosen.

Contradictory to the larger pod, the engine limits of the smaller pod does have a constant power region between 12.6 kn and 13.9 kn, allowing more flexibility in optimization. As shown in Figure 5-8, the final design shows a power of 10.5 kW at 12.6 kn with an unit efficiency of 0.760.

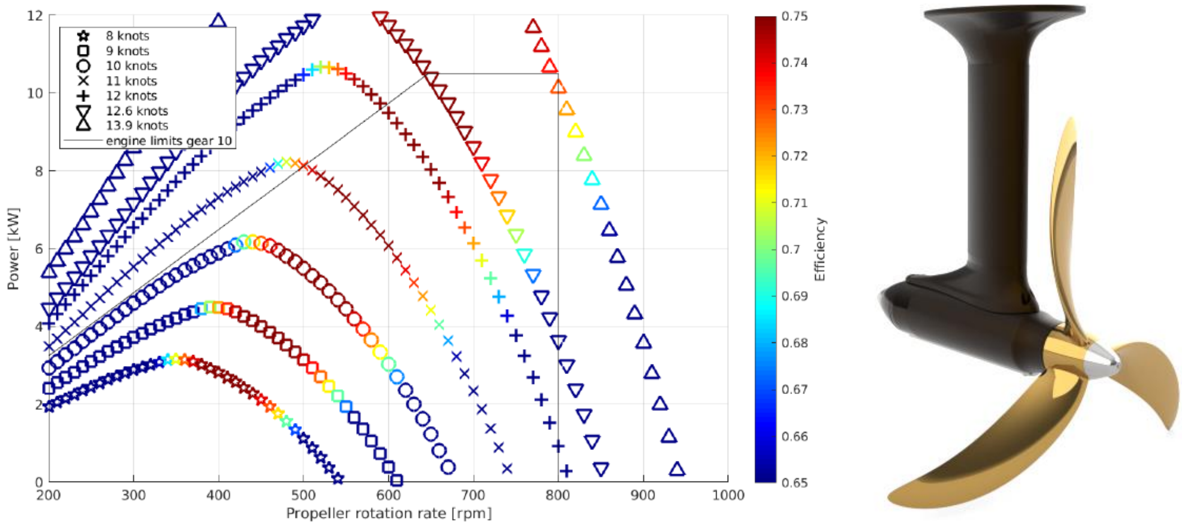

Figure 5-8: *Left: Propeller curves and engine limits 10.5 kW propeller. Right: Dedicated regeneration system 10.5 kW*

6. DISCUSSION

For a hydro-generation device to be successful it needs to be well suited to the overall design of the sailing ship and her intended use. In terms of sizing, the generator should strike the right balance between the amount of electrical power that is required and the amount of power that is available. The available power is defined by the attainable sailing speeds, the diameter of the generator disk and the acceptable speed loss. The use of velocity prediction software to balance aero- and hydromechanics, augmented with hydrogenator polynomial performance data, can provide a clear insight in this. The required output power of the hydro-generator is driven by the ambition level of the use case for the vessel, closely linked to the energy consumption. This can range from:

- Increase battery powered periods during sailing, reducing generator running time.
- Harvesting of excess power during sailing to enable a battery powered period at anchor.
- Harvesting of excess power during sailing to power the vessel during times she cannot be sailed.

Carefully balancing these ambitions with the acceptable consequences requires reliable data and scalable predictions for future solutions.

7. CONCLUSION

In this paper the propeller optimization for two very different solutions on power regeneration was presented. Although each solution has its own field of application and associated cost and objective functions for optimization, this paper shows the applicability of the propeller optimization tool PropArt for different scenarios.

When a propeller would be used for power regeneration, PropArt is able to optimize the propeller geometry for both propulsion and power regeneration mode. It appeared that, when operating in the third quadrant of propeller operation, the propeller geometry can be optimized for both propulsion and regeneration, without clear trade-off.

When a propeller is not used for propulsion, all constraints concerning propulsion are not present, which allows dedicated design for regeneration. This allows smaller blade area and results in higher efficiency. The validation of the propeller design for the dedicated regeneration system with model tests showed a good match between computations and measurements, with a slightly better efficiency measured in the tests.

The results as presented in this paper can be used for a better understanding of the potential output and the impact of regeneration of sailing yachts and ships.

8. ACKNOWLEDGEMENTS

The authors acknowledge Foundationº for the possibility of sharing the results in this paper. The complete report for project zero including polynomials for the assessment of power regeneration can be found on their website [1]

REFERENCES

[1] Foundation0 (2024). Propellor. Creating a combined propulsion and hydro generation system – the journey to success. Available at: https://www.foundationzero.org/insights/propellor (Accessed: 21 October 2024)

[2] T. van Terwisga, J. Bosschers, J. Moulijn. (2019). Propulsion design. MARIN report no. 126.

[3] Cooperative Research Ships (2024). Available at: https://www.crships.org/

[4] Huisman, J. Foeth, E-J. (2017). 'Automated multi-objective optimization of ship propellers'. Fifth International Symposium on Marine Propulsors. Espoo, Finland.

[5] Zhang, X. Zheng, X. Cheng, R. Qiu, J. Jin, Y. (2018). 'A Competitive Mechanism Based Mult-objective Particle Swarm Optimizer with Fast Convergence'. Information Sciences 427, 63-7.

[6] J. Dang, J. Brouwer, R. Bosman and C. Pouw. (2012) 'Quasi-Steady Two-Quadrant Open Water Tests for the Wageningen Propeller C- and D-Series', Proceedings of the 29th ONR, Gothenburg, Sweden.